CHAPTER 3

Observations and Data Analysis

The study of star formation in the galaxy group NGC 4213 by Hα emission detection require precise imaging observations and carefully analyzed. The broad-band filters (B, V and R_C) and narrow-band filters ([S II] and Red-continuum) were used for the imaging observations. The physical characteristics of the sample galaxies can be measured from the broad-band imaging data. We can obtain the information to analyze the star formation of the sample galaxies by equivalent width of Hα ($EW(\mathrm{H}\alpha)$) measurement from narrow-band data images. The detail of the research procedures will be presented in this chapter.

3.1 Photometric Observations and Sample Galaxies

The imaging observations with broad-band filters (B, V and R_C) and narrow-band filters ([S II] and Red-continuum) were carried out from 2.4-m reflecting telescope at Thai National Observatory (TNO). The camera which is used to collect the light of the sample galaxies is Apogee U42 CCD. Its array size is 2048×2048 pixels and pixel size is 13.5×13.5 microns. The field of view of the CCD when connected to the 2.4-m focal length telescope is $4' \times 4'$ approximately. The [S II] filter was applied to cover Hα line of galaxies because the galaxy group has low redshift, as a result, the centered wavelength of Hα shifts into [S II] transmission regions. The continuum subtraction was operated by using observed data through a narrow-band Red-continuum filter. The observations were done on 22 March 2014 with the exposure time for each filter shown in table 3.1. The image layout of the sample galaxies were shown in figure 3.1. However, the raw galaxy images must be calibrated by using image reduction with bias, dark, and flat field images before physical parameters were measured.

Table 3.1: Data observations at Thai National Observatory.

Filters	λ_{eff} (nm)	Date	Exposure Times (s)
B	445	22 March 2014	900
V	551	22 March 2014	600
R_C	658	22 March 2014	300
Red-continuum	645	22 March 2014	900
[S II]	672	22 March 2014	900

For this research, the 11 sample galaxies in galaxy group NGC 4213, centered at the position of R.A. 12h 15m, Dec. 23° 57′ locate in Coma Berenices constellation. The NGC 4213 Group has an average recessional velocity of about 6,821 km s^{-1} ($z \approx 0.02$) with average distance is about 100 Mpc. The NGC 4213 Group was chosen to study because its redshift is appropriate to the limit of the observing instruments which is connected to the 2.4-m telescope at TNO, i.e. bandwidth of filters. Furthermore, the surface brightness of the sample galaxies must be enough to detect by the telescope with the CCD. Moreover, many archive data of sample galaxies; coordinates, velocities and redshifts were accumulated from NASA/IPAC Extragalactic Database (NED) as given by table 3.2.

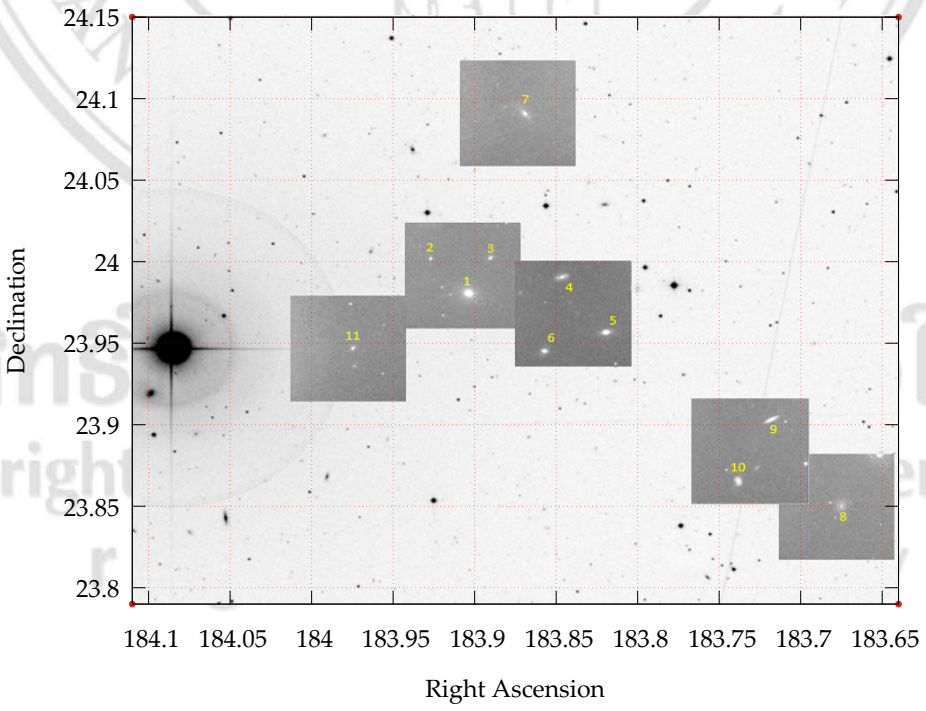

Figure 3.1: The layout of the sample galaxy images, consist of 6 flames.

Table 3.2: The sample galaxies in NGC 4213 Group (from NED Database).

No.	Galaxy Names	Position (J2000)	Redshift
1	NGC 4213	12h15m37.5s +23d58m55s	0.022482
2	2MASX J12154304+2400156	12h15m43.0s +24d00m16s	0.022455
3	2MASX J12153399+2400116	12h15m34.0s +24d00m12s	0.020934
4	2MASX J12152202+2359376	12h15m22.0s +23d59m37s	0.025094
5	IC 0772	12h15m15.9s +23d57m29s	0.022315
6	2MASX J12152523+2356536	12h15m25.2s +23d56m53s	0.022963
7	UGC 07266	12h15m28.9s +24d05m33s	0.023093
8	KUG 1212+241	12h14m41.4s +23d51m10s	0.022225
9	2MFGC 09641	12h14m51.4s +23d54m24s	0.022389
10	2MASX J12145681+2352066	12h14m56.8s +23d52m07s	0.023780
11	2MASX J12155377+2356477	12h15m53.7s +23d56m47s	0.022275

3.2 Zero Points

The reference stars appeared within the galaxy images were measured the instrumental magnitude by `Starlink` software for broad-band filters. The apparent magnitude of the reference stars were obtained from USNO B1 database. After that, the zero point for B-band can be calculated from equation 3.1;

$$zp^{\star}_{\mathrm{B}_i} = m^{\star}_{\mathrm{B}_i} - m^{\star}_{\mathrm{B}_i\mathrm{inst}}, \tag{3.1}$$

where $zp^{\star}_{\mathrm{B}_i}$ is the zero point of reference stars in B-band, $m^{\star}_{\mathrm{B}_i}$ is corresponding to the apparent magnitude in B-band and $m^{\star}_{\mathrm{B}_i\mathrm{inst}}$ represents to the B-band instrumental magnitude of the reference stars. We also use the equation 3.1 for the zero point in V and R filters. Since the most of apparent magnitudes in V-band are not available on USNO B1 catalog, thereby V apparent magnitudes can be calculated by the equation 3.2 which was proposed by Greaves (2003).

$$m^{\star}_{\mathrm{V}_{\mathrm{cal}_i}} = 0.444 m^{\star}_{\mathrm{B}_i} + 0.556 m^{\star}_{\mathrm{R}_i}. \tag{3.2}$$

Due to the reference stars in the data images are not available to designate the zero point for magnitude calibration in some frames. When the zero point of all reference stars were obtained, we will determine an averaged zero point for each broad-band filter. The average zero point for B-band filter is given by

$$ZP^{\star}_{\mathrm{B}} = \frac{\sum_{i=1}^{N} zp^{\star}_{\mathrm{B}_i}}{N}, \tag{3.3}$$

where $ZP^{\star}_{\mathrm{B}}$ is an averaged zero point in B-band, $zp^{\star}_{\mathrm{B}_i}$ is the zero point of each star and N is the total number of the reference stars in all data images. The coordinate of the reference stars, apparent magnitudes, and calculated zero points are listed in the table 3.3.

Since the `Starlink` package provides the error of the instrumental magnitude measurements. Therefore, the averaged zero point that correlated with the magnitude should be estimated the error as follows:

$$\sigma_{ZP^{\star}_{\mathrm{B}}} = \sqrt{\sigma^2_{\mathrm{std},ZP^{\star}_{\mathrm{B}}} + \sigma^2_{\mathrm{av},m^{\star}_{\mathrm{B}_i}}}, \tag{3.4}$$

where

$$\sigma_{\mathrm{std},ZP^{\star}_{\mathrm{B}}} = \sqrt{\frac{\sum_{i=1}^{N}(zp^{\star}_{\mathrm{B}_i} - ZP^{\star}_{\mathrm{B}})^2}{N(N-1)}}, \tag{3.5}$$

and

$$\sigma_{\mathrm{av},m^{\star}_{\mathrm{B}_i}} = \sqrt{\frac{\sum_{i=1}^{N}(\sigma_{m^{\star}_{\mathrm{B}_i\,\mathrm{inst}}})^2}{N}}, \tag{3.6}$$

here $\sigma_{\mathrm{std},ZP^{\star}_{\mathrm{B}}}$ is the standard error of the averaged zero point, $\sigma_{\mathrm{av},m^{\star}_{\mathrm{B}_i}}$ is the averaged error of instrumental magnitude, and $\sigma_{m^{\star}_{\mathrm{B}_i\,\mathrm{inst}}}$ is the error of the instrumental magnitude that is provided by the `Starlink`.

Table 3.3: The reference stars for determine the zero points.

USNO No.	Position (J2000)	$m^{\star}_{\mathrm{B}_i}$	$m^{\star}_{\mathrm{V}_{cal_i}}$	$m^{\star}_{\mathrm{R}_i}$	$m^{\star}_{\mathrm{B}_i\mathrm{inst}}$	$m^{\star}_{\mathrm{V}_i\mathrm{inst}}$	$m^{\star}_{\mathrm{R}_i\mathrm{inst}}$	$zp^{\star}_{\mathrm{B}}$	$zp^{\star}_{\mathrm{V}}$	$zp^{\star}_{\mathrm{R}}$
1139-0191277	12h15m41.57s +23d59m11.1s	18.25	17.00	16.01	-13.19	-14.23	-14.16	31.44	30.17	31.24
1139-0191274	12h15m40.33s +23d58m53.6s	18.37	17.75	17.25	-13.07	-13.69	-13.34	31.44	30.59	31.44
1139-0191278	12h15m41.59s +23d58m28.1s	19.84	19.33	18.92	-11.09	-11.94	-11.54	30.93	30.46	31.26
1139-0191225	12h15m24.80s +23d58m42.9s	20.16	18.88	17.85	-11.35	-12.51	-12.49	31.51	30.34	31.39
1139-0191180	12h15m14.71s +23d56m18.8s	17.87	16.72	15.81	-13.40	-14.63	-14.60	31.27	30.41	31.35
1141-0194020	12h15m32.76s +24d06m42.1s	20.31	18.55	17.14	-11.30	-12.69	-12.92	31.61	30.06	31.24
1138-0191987	12h14m46.62s +23d52m41.3s	15.77	14.73	13.90	-15.77	-17.06	-17.08	31.54	30.98	31.79
1138-0191979	12h14m43.09s +23d51m20.4s	17.69	16.91	16.28	-13.64	-14.56	-14.39	31.33	30.67	31.47
1138-0191975	12h14m42.43s +23d50m46.1s	19.05	18.33	17.75	-12.40	-13.16	-12.92	31.45	30.67	31.48
1138-0191938	12h14m35.65s +23d50m26.1s	19.95	19.20	18.60	-12.03	-12.58	-12.21	31.98	30.81	31.78
1138-0192021	12h14m49.35s +23d54m17.8s	18.13	17.55	17.09	-13.33	-13.40	-13.13	31.46	30.22	30.95
1138-0191987	12h14m46.62s +23d52m41.3s	15.77	14.73	13.90	-15.79	-16.67	-16.82	31.56	30.72	31.40
1138-0192021	12h14m58.56s +23d52m34.1s	18.13	17.55	17.09	-13.33	-13.40	-13.13	31.46	30.22	30.95
1139-0191313	12h15m53.79s +23d58m27.6s	17.07	16.56	16.15	-14.30	-14.85	-14.51	31.37	30.66	31.40
1139-0191300	12h15m49.50s +23d55m47.8s	18.20	17.05	16.13	-13.12	-14.23	-14.29	31.32	30.42	31.28
							Average	31.45	30.49	31.36

3.3 B_{25} Isophotes of the Sample Galaxies

B_{25} isophote is a contour of 25 mag arcsec^{-2} surface brightness of B-band filter around the galaxy center. This contour is corresponding to about of one-tenth surface brightness of the night sky brightness (Redman, 1936). The isophotes can be obtained by using the ESP package of Starlink software. Three parameters of the isophotes are used to measure size and orientation of the galaxies in the space. Importantly, the parameters are used to specify the aperture in the Starlink for apparent magnitude and flux count measurements. The semi-major axis in pc unit were obtained by the correlation of averaged distance of galaxy group and angular size of each galaxy. The semi-major axis, ellipticity, and position angle are listed in table below:

Table 3.4: The B_{25} isophotes.

Galaxy No.	Semi-major axis (kpc)	Ellipticity	Position angle (°)
1	16.78	0.63	72
2	4.357	0.65	172
3	5.290	0.59	139
4	8.206	0.84	102
5	9.054	0.86	100
6	5.595	0.49	121
7	13.48	0.88	44
8	8.336	0.59	151
9	9.732	0.95	114
10	6.109	0.66	177
11	4.222	0.57	36

3.4 Measurement of Magnitudes and Color Indices

Magnitude of galaxy measurement is used to describe its physical properties. However, the extended objects as galaxies are difficult to define their boundaries against the night sky background. So, the used aperture is essentially required to cover the light as much as possible and be well defined. According to the convention of the second Reference Catalogue of Bright Galaxies (de Vaucouleurs et al., 1976), the B_{25} isophotes were used to define the standard aperture size and also used to define aperture in this research.

3.4.1 Apparent magnitudes

Apparent magnitudes of galaxies are measured by the Graphical Astronomy and Image Analysis (GAIA) package of the Starlink. The defined elliptical aperture size and averaged zero points were applied in this procedure. The number of photon counts will be separated in two regions, i.e. aperture region and annular sky region. The photon counts within the aperture region will be subtracted by the photon counts within the annular sky region. Then, the instrumental magnitudes are computed together with zero points that are applied to calibrate the magnitudes as follow in equation 3.7-3.9. Theses steps which are automatically operated with GAIA package.

$$B' = ZP^{\star}_{\mathrm{B}} + B_i, \tag{3.7}$$

$$V' = ZP^{\star}_{\mathrm{V}} + V_i, \tag{3.8}$$

$$R' = ZP^{\star}_{\mathrm{R}} + R_i, \tag{3.9}$$

where B', V' and R' are the calibrated apparent magnitudes of the sample galaxies in B, V and R filters. B_i, V_i and R_i are the instrumental magnitudes in B, V and R filters, respectively.

3.4.2 Galactic extinction correction

The space between the galaxies and the observer fills with interstellar or intragalactic medium. This factor can affect to the magnitude measurement. Therefore, the apparent magnitude that we obtained from the GAIA package must be corrected by the galactic extinction. The available galactic extinction of B, V and R bands from NED are given in table 3.5. The apparent magnitude of the sample galaxies were increased (brightness is decreasing) by the effect of galactic extinction. The extincted correction value will compensate the galaxy brightness as given by equation 3.10-3.12.

$$B = B' - A_{\mathrm{B}}, \tag{3.10}$$

$$V = V' - A_{\mathrm{V}}, \tag{3.11}$$

$$R = R' - A_{\mathrm{R}}, \tag{3.12}$$

where B, V and R are the extinction corrected apparent magnitudes, while A_{B}, A_{V} and A_{R} are the galactic extinction of B, V and R bands for each galaxies.

Table 3.5: The galactic extinction of the sample galaxies in B, V and R bands from NED.

Galaxy No.	Galactic Extinctions		
	A_{B}	A_{V}	A_{R}
1	0.135	0.102	0.081
2	0.128	0.097	0.077
3	0.134	0.101	0.080
4	0.143	0.108	0.085
5	0.151	0.114	0.090
6	0.143	0.108	0.086
7	0.120	0.091	0.072
8	0.147	0.112	0.088
9	0.150	0.114	0.090
10	0.144	0.109	0.086
11	0.124	0.094	0.074

Equation 3.13 shows the uncertainty of the apparent magnitudes in B-band (σ_B). It includes the error of the averaged zero point ($\sigma_{ZP^{\star}_{\mathrm{B}}}$) (equation 3.4) and the uncertainty of the instrumental magnitudes (σ_{B_i}) provided by the `GAIA` package.

$$\sigma_B = \sqrt{\sigma^2_{ZP^{\star}_{\mathrm{B}}} + \sigma^2_{\mathrm{B}_i}}. \tag{3.13}$$

The uncertainties of the apparent magnitudes for V and R bands are calculated in the same way of B-band and presented in table 3.6.

Table 3.6: The apparent magnitudes of the sample galaxies in B, V and R bands.

Galaxy No.	B	σ_B	V	σ_V	R	σ_R
1	14.26	0.06	13.19	0.06	12.44	0.07
2	17.37	0.06	16.36	0.06	15.66	0.07
3	16.83	0.06	15.81	0.06	15.10	0.07
4	16.70	0.06	15.50	0.06	14.73	0.07
5	15.57	0.06	14.46	0.06	13.71	0.07
6	16.44	0.06	15.38	0.06	14.64	0.07
7	15.62	0.06	14.78	0.06	14.16	0.07
8	16.11	0.06	15.36	0.06	14.83	0.07
9	16.07	0.06	15.39	0.06	14.53	0.07
10	16.39	0.06	15.96	0.06	15.20	0.07
11	17.11	0.06	16.14	0.06	15.45	0.07

3.4.3 Absolute magnitudes

Astronomers have defined the standard distance at 10 pc to consider the brightness of celestial objects for same distance. The apparent magnitudes and the averaged distance of the galaxy group are used to measure the absolute magnitudes by the equation 3.14-3.16 for B, V and R bands, respectively.

$$M_{\mathrm{B}} = B - 5\log d + 5, \tag{3.14}$$

$$M_{\mathrm{V}} = V - 5\log d + 5, \tag{3.15}$$

$$M_{\mathrm{R}} = R - 5\log d + 5. \tag{3.16}$$

M_{B}, M_{V} and M_{R} are the absolute magnitudes of B, V and R bands, respectively. While d is the averaged distance of the galaxy group. The absolute magnitudes and their errors are shown in table 3.7.

Table 3.7: The absolute magnitudes of the sample galaxies in B, V and R bands.

Galaxy No.	M_{B}	$\sigma_{M_{\mathrm{B}}}$	M_{V}	$\sigma_{M_{\mathrm{V}}}$	M_{R}	$\sigma_{M_{\mathrm{R}}}$
1	-20.75	0.06	-21.82	0.06	-22.57	0.07
2	-17.64	0.06	-18.66	0.06	-19.35	0.07
3	-18.19	0.06	-19.21	0.06	-19.91	0.07
4	-18.31	0.06	-19.51	0.06	-20.28	0.07
5	-19.44	0.06	-20.55	0.06	-21.30	0.07
6	-18.57	0.06	-19.64	0.06	-20.38	0.07
7	-19.39	0.06	-20.24	0.06	-20.85	0.07
8	-18.90	0.06	-19.66	0.06	-20.18	0.07
9	-18.94	0.06	-19.63	0.06	-20.48	0.07
10	-18.62	0.06	-19.05	0.06	-19.82	0.07
11	-17.90	0.06	-18.87	0.06	-19.56	0.07

3.4.4 Color index of galaxies

The color index is a numerical expression that represents the color of sky objects. The index correlates with the temperature and spectral types. The color index was calculated from the difference in magnitudes between two wavebands, in this case, $B-V$, $B-R$ and $V-R$ color indices. Furthermore, the errors of the color indices were computed by using the following equation:

$$\sigma_{B-V} = \sqrt{\sigma_B^2 + \sigma_V^2}, \tag{3.17}$$

$$\sigma_{B-R} = \sqrt{\sigma_B^2 + \sigma_R^2}, \tag{3.18}$$

$$\sigma_{V-R} = \sqrt{\sigma_V^2 + \sigma_R^2}. \tag{3.19}$$

Table 3.8 lists the color indices and their errors of the sample galaxies. The correlation among the color index with the physical parameters (e.g. morphology, $EW(\mathrm{H}\alpha)$) will be analyzed to understand the characteristic of the galaxies in the next sections.

Table 3.8: The color indices of the sample galaxies.

Galaxy No.	$B-V$	σ_{B-V}	$B-R$	σ_{B-R}	$V-R$	σ_{V-R}
1	1.07	0.09	1.82	0.09	0.75	0.09
2	1.02	0.09	1.72	0.09	0.70	0.09
3	1.02	0.09	1.73	0.09	0.71	0.09
4	1.20	0.09	1.96	0.09	0.76	0.09
5	1.11	0.09	1.86	0.09	0.75	0.09
6	1.07	0.09	1.81	0.09	0.74	0.09
7	0.84	0.09	1.45	0.09	0.61	0.09
8	0.76	0.09	1.28	0.09	0.53	0.09
9	0.68	0.09	1.54	0.09	0.86	0.09
10	0.43	0.09	1.20	0.09	0.76	0.09
11	0.96	0.09	1.66	0.09	0.70	0.09

3.5 Classification of Morphological Type of Galaxies

Morphological type of the sample galaxies in this research were classified into Hubble system and de Vaucouleurs T-type. The dwarf elliptical galaxies were classified as `dE` and identified to be an extra T-type -7. There are 11 sample galaxies in this research, consisting of 2 ellipticals, 2 lenticulars and 7 spirals as shown in table 3.9. The morphological type will be used to analyze for dependence between star formation and galaxy evolution.

Table 3.9: The morphological type and T-type of the sample galaxies.

Galaxy Names.	Morphological Type		T-Type
	Goldmine	This research	
1	E-E/S0	E^+	-4
2	E-E/S0	dE	-7
3	E-E/S0	Sm	9
4	S0a-S0/Sa	SBb	3
5	E-E/S0	$S0^-$	-3
6	S0a-S0/Sa	SBa	1
7	Sa	Sab	2
8	Sab	Scd	6
9	S0	S0/a	0
10	Sa	SBb	3
11	S0a-S0/Sa	Sb	3

3.6 Calculation of $\mathrm{H}\alpha + [\mathrm{N\,II}]$ Equivalent Width ($EW(\mathrm{H}\alpha + [\mathrm{N\,II}])$)

The young massive star formation activity in a galaxy can be traced by $\mathrm{H}\alpha$ emission line from H II regions heated up by these massive stars. The amount of $\mathrm{H}\alpha$ emission is reported in term of equivalent width. Nevertheless, $EW(\mathrm{H}\alpha)$ determination has some procedures needed to calculate the calibrated factors to convert the narrow-band flux counts of the galaxies to be the $EW(\mathrm{H}\alpha)$.

3.6.1 Continuum ratio

Because of the $\mathrm{H}\alpha$ luminosity flux counts were detected by the [S II] filter for the low redshift galaxies which includes continuum counts. Hence the narrow-band luminosity flux counts of reference stars are applied to calculate the continuum-ratio (CR). Under two assumptions, the stars do not have $\mathrm{H}\alpha$ emission line, so the stars should emit only continuum in the narrow band filters, and the continuum-ratio of the reference stars should be constant all over the spectral types. The continuum-ratio shown in equation 3.20 is the scale factor that will be used to remove the continuum counts from the [S II] flux counts of the sample galaxies.

$$CR_i = \frac{C^{\star}_{[\mathrm{S\,II}]}}{C^{\star}_{\mathrm{Red-con}}}. \tag{3.20}$$

CR_i is the continuum-ratio of each reference star, $C^{\star}_{[\mathrm{S\,II}]}$ refers to the [S II] flux count of reference stars, while $C^{\star}_{\mathrm{Red-con}}$ is corresponding to the flux count of reference stars in the Red-continuum filter.

Due to the reference stars in the data images are not available to provide the continuum-ratio for some frames. We will determined an averaged continuum-ratio for all data images by following the equation:

$$CR = \frac{\sum_{i=1}^{N} CR_i}{N}, \tag{3.21}$$

and

$$\sigma_{CR} = \sqrt{\frac{\sum_{i=1}^{N}(CR_i - CR)}{N(N-1)}}, \tag{3.22}$$

where CR is the averaged continuum-ratio, σ_{CR} represents its uncertainty, and N is the number of the reference stars. After that, the continuum flux counts of the sample galaxies will be calibrated to be

$$C_{\mathrm{c}} = CR \times C_{\mathrm{Red-con}}, \tag{3.23}$$

where C_{c} refer to the continuum counts and $C_{\mathrm{Red-con}}$ is the flux counts of each galaxy in Red-continuum band. While the error of the continuum counts ($\sigma_{C_{\mathrm{c}}}$) shown in equation 3.24 consists of two errors. One is continuum-ratio error (σ_{CR}), and the other is error of the Red-continuum counts of the galaxies ($\sigma_{C_{\mathrm{Red-con}}}$) which are provided by equation 3.25.

$$\sigma_{C_{\mathrm{c}}} = C_{\mathrm{c}}\sqrt{\left(\frac{\sigma_{CR}}{CR}\right)^2 + \left(\frac{\sigma_{C_{\mathrm{Red-con}}}}{C_{\mathrm{Red-con}}}\right)^2}, \tag{3.24}$$

while

$$\sigma_{C_{\mathrm{Red-con}}} = \sqrt{\frac{C_{\mathrm{Red-con}}}{k}}, \tag{3.25}$$

where k is corresponding to the e^-/ADU gain of CCD camera, which k equal to 1.25.

3.6.2 Hα + [N II] emission line counts

In this research, Hα emission line (λ = 6563 Å) associated with [N II] lines, 6548 Å and 6583 Å were detected when we used [S II] band filter. Due to [S II] band signal was included of Hα + [N II] emission counts and continuum counts. In order to calculate the Hα + [N II] emission counts, the equation 3.26 was applied after we obtain both the

continuum flux counts of the galaxies from § 3.6.1 and the flux counts in [S II] band

$$C_{\mathrm{H}\alpha+[\mathrm{N\,II}]} = C_{[\mathrm{S\,II}]} - C_{\mathrm{c}}, \tag{3.26}$$

where $C_{\mathrm{H}\alpha+[\mathrm{N\,II}]}$ is the $\mathrm{H}\alpha + [\mathrm{N\,II}]$ flux counts and $C_{[\mathrm{S\,II}]}$ is the [S II] flux counts. The uncertainty of $\mathrm{H}\alpha + [\mathrm{N\,II}]$ flux counts $\sigma_{C_{\mathrm{H}\alpha+[\mathrm{N\,II}]}}$ is:

$$\sigma_{C_{\mathrm{H}\alpha+[\mathrm{N\,II}]}} = \sqrt{\sigma^2_{C_{[\mathrm{S\,II}]}} + \sigma^2_{C_{\mathrm{c}}}}, \tag{3.27}$$

while

$$\sigma_{C_{[\mathrm{S\,II}]}} = \sqrt{\frac{C_{[\mathrm{S\,II}]}}{k}}. \tag{3.28}$$

3.6.3 $\mathrm{H}\alpha + [\mathrm{N\,II}]$ equivalent width and signal to noise ratio

The $\mathrm{H}\alpha + [\mathrm{N\,II}]$ equivalent width ($EW(\mathrm{H}\alpha + [\mathrm{N\,II}])$) is a parameter that can be used to measure the strength of a $\mathrm{H}\alpha + [\mathrm{N\,II}]$ spectral line. It is defined as the width of a box reaching up to the continuum that has the same area as the normalized spectral line (Carroll and Ostlie, 2014). Moreover, it is an indicator that will be used to examine the star formation in the galaxies. $EW(\mathrm{H}\alpha + [\mathrm{N\,II}])$ was calculated as the following equation (Gavazzi et al., 2006; Kriwattanawong et al., 2011).

$$EW(\mathrm{H}\alpha + [\mathrm{N\,II}]) = \frac{\int T_n(\lambda) d\lambda}{T_n(6563(1+z))} \times \frac{C_{\mathrm{H}\alpha+[\mathrm{N\,II}]}}{C_{\mathrm{c}}}, \tag{3.29}$$

where $T_n(\lambda)$ is the [S II] filter transmissivity, z is the redshift of the galaxies. Typically, the filters have the transmissivity as a function of wavelength. There are many wavelengths that have higher transmissivity, while some wavelengths are lower. In order to calibrate $EW(\mathrm{H}\alpha + [\mathrm{N\,II}])$ of the galaxies redshifted into an unknown wavelength, the term of $T_n(6563(1+z))$ is applied to compensate some flux counts lost by filter efficiency. The transmissivity of the [S II] filter is shown in figure 3.2. The highest of the profile has the transmissivity is about 93% at $\lambda = 6730$ Å. Furthermore, the signal to noise ratio, S/N, was used to verify the significance of $EW(\mathrm{H}\alpha + [\mathrm{N\,II}])$ value. The S/N was determined as follows:

$$S/N = \frac{C_{\mathrm{H}\alpha+[\mathrm{N\,II}]}}{\sigma_{C_{\mathrm{H}\alpha+[\mathrm{N\,II}]}}}. \tag{3.30}$$

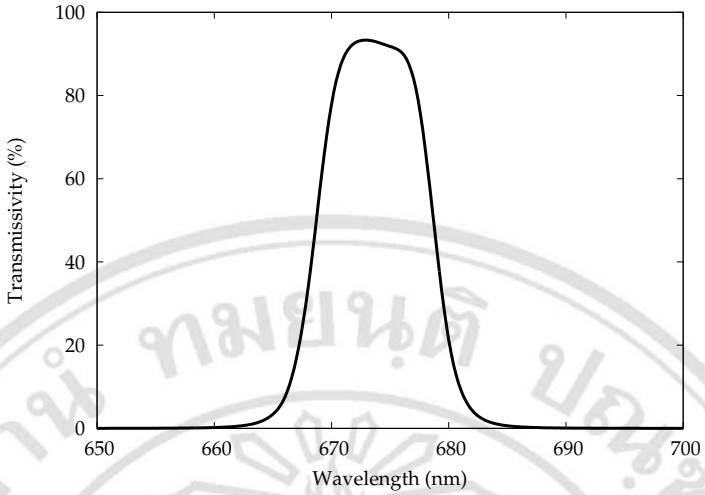

Figure 3.2: Transmissivity profile of the [S II] filter that were used in this research.

In this research we needed the S/N value of photon signal more than 3.0 which representing more than 99% statistical significance. Since the $EW(\mathrm{H}\alpha + [\mathrm{N\,II}])$ is proportional to $C_{\mathrm{H}\alpha+[\mathrm{N\,II}]}$ as equation 3.29. Therefore, the equation 3.30 may be expressed as equation:

$$S/N = \frac{EW(\mathrm{H}\alpha + [\mathrm{N\,II}])}{\sigma_{EW(\mathrm{H}\alpha+[\mathrm{N\,II}])}}. \tag{3.31}$$

Thus the uncertainties of the $EW(\mathrm{H}\alpha + [\mathrm{N\,II}])$ are determined by equation 3.32 after we obtained the S/N and $EW(\mathrm{H}\alpha + [\mathrm{N\,II}])$. The results of these calculations are listed in table 3.10.

$$\sigma_{EW(\mathrm{H}\alpha+[\mathrm{N\,II}])} = \frac{EW(\mathrm{H}\alpha + [\mathrm{N\,II}])}{S/N}. \tag{3.32}$$

Table 3.10: The $\mathrm{H}\alpha + [\mathrm{N\,II}]$ equivalent width and signal to noise ratio.

Galaxy No.	$EW(\mathrm{H}\alpha + [\mathrm{N\,II}])$ (Å)	$\sigma_{EW(\mathrm{H}\alpha+[\mathrm{N\,II}])}$(Å)	S/N
1	3.608	1.259	2.865
2	1.733	1.321	1.312
3	1.465	1.466	0.999
4	11.77	1.22	9.670
5	4.688	1.265	3.706
6	5.084	1.259	4.038
7	7.953	1.239	6.420
8	12.41	1.30	9.550
9	6.365	1.270	5.011
10	15.58	1.23	12.66
11	6.472	1.298	4.986

3.7 Calculation of Star Formation Rates

In § 3.6.2 mentioned that the [S II] flux counts are contained with the Hα and [N II] emission line counts. So, the luminosity flux counts of Hα that applied to calculate the $EW(\mathrm{H}\alpha)$ are contaminated with [N II] counts. However, the luminosity flux counts must be corrected for the [N II] contamination before approximate the star formation rate (SFR) in the sample galaxies.

3.7.1 Correction of [N II] to Hα fluxes

The astronomers have proposed the [N II] correction ratio to improve the Hα fluxes. For example, Kennicutt (1983) and Kennicutt and Kent (1983) demonstrated that the averaged $H\alpha/\left(H\alpha+[NII]\right)$ ratio was reasonably constant, ranges 0.75(0.12) for spiral galaxies and 0.93(0.05) for the irregulars. James et al. (2005) studied the two corrections applied to estimate star formation rate of the 5 sample galaxies, one correction for [N II] contamination and the other for intra-galactic extinction. They suggested that the $H\alpha/\left(H\alpha+[NII]\right)$ ratio was about 0.823. Furthermore, Lee et al. (2009) used 300 star-forming galaxies to study the star formation and they proposed that the correction ratio is estimated from the luminosity-metallicity relation of galaxies, the average correlation between $[N\,II]\lambda6583/H\alpha$ and M_{B}. The integrated spectroscopic data set was used to derive the scaling relationship;

$$\log\left(\frac{[N\,II]_{\lambda6583}}{H\alpha}\right) = (-0.173\pm0.007)M_{\mathrm{B}} - (3.903\pm-0.137) \quad \text{if } M_{\mathrm{B}} > -20.3, \tag{3.33}$$

$$\frac{[NII]_{\lambda6583}}{H\alpha} = 0.54 \quad \text{if } M_{\mathrm{B}} \leqslant -20.3. \tag{3.34}$$

Equation 3.33 and 3.34 indicated that the $[N\,II]\lambda6583/H\alpha$ ratio is depending on the absolute magnitude in B-band. Otherwise, the [N II] correction ratio can be derived by

$$\frac{H\alpha}{H\alpha+[NII]} = \frac{1}{1+\left(\frac{[NII]}{H\alpha}\right)}. \tag{3.35}$$

Table 3.11: The estimation of the [N II] correction ratio.

Galaxy No.	M_B	$H\alpha/\left(H\alpha + [NII]\right)$
1	-20.75	0.649
2	-17.64	0.877
3	-18.19	0.851
4	-18.31	0.844
5	-19.44	0.776
6	-18.57	0.831
7	-19.39	0.779
8	-18.90	0.811
9	-18.94	0.809
10	-18.62	0.828
11	-17.90	0.865

From the previous study, the astronomers have estimated the star formation rate in the galaxies by using the Hα luminosity. The luminosity is the intrinsic property of the radiative sky object, i.e. the energy emitted per second. Actually, the brightness of the object measured in term of radiative flux. The radiative flux is the total amount of energy of all wavelengths that crosses a unit area oriented perpendicular to the line of sight per unit time, in unit W m^{-2}. Whereas the Hα flux counts that were obtained from equation 3.26 are the amount detected photons from CCD camera in the unit of counts, Hα flux counts should be scaled by using the flux scale parameter and [N II] correction ratio to obtain the Hα fluxes as:

$$f_{\mathrm{H}\alpha} = (flux\,scale\,parameter)\left(\frac{H\alpha}{H\alpha + [NII]}\right) C_{\mathrm{H}\alpha+[\mathrm{N\,II}]}. \tag{3.36}$$

$flux\,scale\,parameter$ was defined by the ratio of the available Hα flux of UCG 07266 galaxy from NED to its Hα flux counts. The flux scale parameter was designated in the unit W m^{-2}count^{-1}. Otherwise, $C_{\mathrm{H}\alpha+[\mathrm{N\,II}]}$ refer to the raw flux count of Hα + [N II]. The uncertainty of the Hα fluxes was given as:

$$\sigma_{f_{\mathrm{H}\alpha}} = \frac{f_{\mathrm{H}\alpha}}{S/N}. \tag{3.37}$$

Table 3.12 represents the comparison between the raw Hα + [N II] flux counts and the Hα flux counts which are improved by the [N II] correction ratio of two methods (i.e. James et al., 2005; Lee et al., 2009). The error of corrected Hα flux count in the column 5 was

still calculated by the equation 3.27. It was found that, the Hα flux counts are a little difference compared with the whole signals.

This research have chosen Lee et al. (2009) method to approximate the [N II] correction ratio, due to it is newer and the ratio can be considered by given B-band absolute magnitudes in § 3.4.3. In addition, columns 6 and 7 have shown the Hα fluxes and their errors, which will then be used to estimate the SFR.

Table 3.12: The [N II] corrected Hα flux counts and fluxes

Galaxy No.	$C_{\mathrm{H}\alpha+[\mathrm{N\,II}]}$	$C_{\mathrm{H}\alpha_{\mathrm{J}}}$	$C_{\mathrm{H}\alpha_{\mathrm{L}}}$	$\sigma_{C_{\mathrm{H}\alpha}}$	$f_{\mathrm{H}\alpha}$ $\left(10^{-17}\,\mathrm{W\,m^{-2}}\right)$	$\sigma_{f_{\mathrm{H}\alpha}}$ $\left(10^{-17}\,\mathrm{W\,m^{-2}}\right)$
1	89385	73564	58042	31199	7.071	2.468
2	1798	1480	1577	1371	0.192	0.146
3	3059	2517	2603	3061	0.317	0.317
4	42142	34683	35586	4358	4.335	0.448
5	38615	31780	29970	10419	3.651	0.985
6	18758	15438	15582	4645	1.898	0.470
7	49461	40706	38545	7704	4.696	0.731
8	40680	33479	33001	4260	4.020	0.421
9	32506	26752	26282	6486	3.202	0.639
10	45553	37490	37707	3598	4.594	0.363
11	10762	8857	9306	2158	1.134	0.227

3.7.2 Hα luminosity and star formation rates

Hα luminosities, $L_{\mathrm{H}\alpha}$ can be calculated from Hα fluxes by multiplying by $4\pi d^2$ as given equation:

$$L_{\mathrm{H}\alpha} = 4\pi d^2 f_{\mathrm{H}\alpha}, \tag{3.38}$$

where d refers to the average distance of the galaxy group, meanwhile the luminosity uncertainties can be calculated by

$$\sigma_{L_{\mathrm{H}\alpha}} = \frac{L_{\mathrm{H}\alpha}}{S/N}. \tag{3.39}$$

For this research, the star formation rates are estimated from Hα luminosities using the same equation as James et al. (2004):

$$SFR(\mathrm{M_\odot yr^{-1}}) = 7.94 \times 10^{-35} L_{\mathrm{H}\alpha}\,(\mathrm{W}), \tag{3.40}$$

here SFR is in unit of $M_{\odot}yr^{-1}$ and Hα luminosities are in unit of W, while, the error of the SFR will be determined in the same way as equation 3.37 and 3.39, i.e. SFR divided by S/N.

In another way, the comparison about the rate of star formation activities in star forming galaxies may be defined by the star formation rate per unit mass ($nSFR$) (see § 3.8.1). We found that it may have some possible correlation with the morphological type.

Table 3.13: The Hα luminosities and star formation rates.

Galaxy No.	$L_{H\alpha}$ $(10^5\,L_{\odot})$	$\sigma_{L_{H\alpha}}$ $(10^5\,L_{\odot})$	SFR $(M_{\odot}yr^{-1})$	σ_{SFR} $(M_{\odot}yr^{-1})$	$nSFR$ $(10^{-12}yr^{-1})$	σ_{nSFR} $(10^{-12}yr^{-1})$
1	223.258	77.926	0.679	0.237	0.245	0.232
2	6.065	4.624	0.018	0.014	0.309	0.360
3	10.013	10.021	0.030	0.030	0.259	0.346
4	136.881	14.155	0.416	0.043	3.023	2.679
5	115.278	31.104	0.350	0.095	0.636	0.586
6	59.937	14.843	0.182	0.045	0.969	0.886
7	148.261	23.094	0.451	0.070	0.866	0.774
8	126.938	13.292	0.386	0.040	1.362	1.207
9	101.095	20.173	0.307	0.061	1.027	0.927
10	145.041	11.456	0.441	0.035	2.198	1.943
11	35.794	7.179	0.109	0.022	1.310	1.183

In the columns 2 and 3 of the table 3.13 show the Hα luminosities and its errors in the unit of $10^5 L_{\odot}$, columns 4 and 5 represent the star formation rates and its errors in $M_{\odot}yr^{-1}$ unit, and columns 6 and 7 refer to the $nSFR$ and its errors.

3.8 Estimation of Tidal Interaction Perturbation

Generally, galaxies that are contained in the galaxy clusters or galaxy groups will be interacted from neighboring cluster members. The tidal interaction is one of the interactions which can perturb star formation in the galaxies. The different environment can affect the evolution of galaxies into various morphological types, and led to describe the structure of the galaxy cluster in the future. For the research, we will estimate a possibility of the tidal interaction perturbation act on the group galaxies.

3.8.1 Mass of the sample galaxies

Girardi et al. (2002) had suggested the mass-luminosity relation to determine the mass of the galaxies from studying mass to light ratio of galaxies in small groups to rich clusters. Equation 3.41 is interpreted that the galaxy masses will increase faster than their luminosities (Girardi et al., 2002). But in this research, this relation can still be used, although Girardi et al. (2002) claimed that, the relation might be insufficient to explain the mass-luminosity relation in such a wide dynamical range, from very rich clusters to poor groups.

$$M_{\text{gal}} = 10^{-1.596\pm0.381}\left(\frac{L_{\text{B}}}{L_{\text{B},\odot}}\right)^{1.338\pm0.033}, \tag{3.41}$$

where M_{gal} is the galaxy mass in the $\text{M}_\odot$ unit, $L_{\text{B},\odot}$ corresponds to the solar luminosity in B-band, and L_{B} refers to the luminosity in B-band of the galaxies.

The luminosity flux of the sun in B-band should be known before the B-band luminosity will be calculated from the elementary photometry equations (i.e. equation 2.7 to 2.9). Binney and Merrifield (1998) had provided the absolute B magnitude of the sun 5.48 and derived the flux density in B-band of the sun equal to 1.094×10^{-12} W m^{-2}Hz^{-1}. Therefore, the energy emitted per second at the distance 1 A.U. is 2.072×10^{17} W, where the B-band effective frequency is equal to 6.74×10^{14} Hz. From the distance modulus and the relationship between magnitude and flux density, the luminosity of the galaxies can be calculated by equation:

$$L_{\text{B}} = L_{\text{B},\odot}\left(\frac{d^2}{d_\odot^2}\right)10^{-(B-B_\odot)/2.5}, \tag{3.42}$$

where d represents the averaged distance of the galaxy group, $d_\odot$ refer to the distance of the sun from the Earth in the same unit of d, B is the B-band apparent magnitude of the galaxies, and B-band apparent magnitude of the sun is represented by $B_\odot$. The uncertainty of the galaxy mass, $\sigma_{M_{\text{gal}}}$ is derived from equation 3.41. The error of the power number of luminosity in equation 3.41, 0.033 is much smaller than 1.338, means that the power number of luminosity is relatively constant, then yields

$$\sigma_{M_{\text{gal}}} = M_{\text{gal}}\sqrt{(0.381\ln 10)^2 + 1.338^2\left(\frac{\sigma_{L_{\text{B}}}}{L_{\text{B}}}\right)^2}, \tag{3.43}$$

and

$$\sigma_{L_{\rm B}} = L_{\rm B}\sqrt{\sigma_B^2\left(\frac{\ln 10}{-2.5}\right)^2}, \tag{3.44}$$

here $\sigma_{L_{\rm B}}$ is the error of the B-band luminosity of the galaxies, while the error of $L_{B,\odot}, d, d_\odot$, and $B_\odot$ are assumed negligible factors. The luminosities and the estimated mass of the galaxies with their errors were shown in table 3.14.

Table 3.14: The B-band luminosities and estimated mass of the galaxies.

Galaxy No.	$L_{\rm B}$ $(10^{36}\,{\rm W})$	$\sigma_{L_{\rm B}}$ $(10^{36}\,{\rm W})$	$M_{\rm gal}$ $(10^{11}\,{\rm M}_\odot)$	$\sigma_{M_{\rm gal}}$ $(10^{11}\,{\rm M}_\odot)$
1	6.445	0.343	27.75	24.43
2	0.366	0.020	0.597	0.525
3	0.606	0.033	1.173	1.033
4	0.683	0.036	1.376	1.211
5	1.925	0.103	5.509	4.849
6	0.862	0.046	1.881	1.655
7	1.845	0.099	5.204	4.581
8	1.171	0.063	2.834	2.494
9	1.220	0.065	2.992	2.633
10	0.904	0.048	2.005	1.765
11	0.468	0.025	0.830	0.731

3.8.2 Mass of the galaxy group

In this research, there are only 11 sample galaxies in NGC 4213 Group that were observed by the TNO telescope. Otherwise, Gavazzi et al. (2013) proposed that the NGC 4213 Group was contained by 26 galaxy members. Moreover, NED has given the radius of NGC 4213 Group of about 18 arcminutes ($\approx$ 526.2 kpc). Thus estimation of the galaxy group mass should be considered all group membership galaxies. The available data of the NGC 4213 Group members are given in table E.1.

Since the redshift measurement for a galaxy is included of two factors, one is the overall Hubble flow, and other is the peculiar, gravitaionally induced velocity of the galaxies in side the cluster (Phillipps, 2005). The mass of the galaxy group can be estimated

from the velocity dispersion, σ_r, which is defined by the distribution of velocities of individual galaxies that are measured by their Doppler shifts as follows:

$$\sigma_r = \sqrt{\frac{\sum_{i=1}^{N} v_{\text{pec},i}^2}{N}}, \tag{3.45}$$

where N is the number of galaxies in the group, while $v_{\text{pec},i}$ represents the peculiar velocity of each galaxy, as defined by the equation 3.46.

$$v_{\text{pec},i} \simeq \frac{cz_i - cz_{\text{group}}}{1 + z_{\text{group}}}, \tag{3.46}$$

here c is the speed of electromagnetic waves in vacuum, z_i refers to the redshift of individual galaxies, and z_{group} corresponds to the redshift of the galaxies group from NED. After that, Phillipps (2005) used the common virial theorem to derive the total group mass as equation,

$$M_{\text{group}} \simeq 7 \times 10^{14} \left(\frac{R_{eff}}{1\text{Mpc}}\right) \frac{\sigma_r^2}{1000\text{km s}^{-1}}, \tag{3.47}$$

where M_{group} is the virial mass of the galaxy group, R_{eff} refers to the effective radius of the group, and σ_r is calculated from equation 3.45. By the way, due to in the research can not observe all galaxies in the NGC 4213 Group, so the error of the group mass will be generated via bootstrapping techniques of 10000 iterations to obtain the new significant data of the group membership.

3.8.3 Perturbation parameters

Due to the tidal interactions resemble the main morphological transformation mechanism of spirals to S0s and might be boosted star formation in group galaxies. So, the good indicator of tidal interaction between galaxy-cluster, galaxy-group, or galaxy-galaxy is the circumnuclear emission in the galaxy either with bar structures or morphological disturbances. Boselli and Gavazzi (2006) and Byrd and Valtonen (1990) provided the parameter to describe the efficiency of the tidal interaction between galaxy-galaxy and galaxy-cluster that were applied in the research. They can be quantified by the perturbation parameter, defined as

$$P_{\text{gg}} = \left(\frac{M_{\text{comp}}}{M_{\text{gal}}}\right) \left(\frac{d}{r_{\text{gal}}}\right)^{-3}, \tag{3.48}$$

and

$$P_{\text{gc}} = \left(\frac{M_{\text{group}}}{M_{\text{gal}}}\right)\left(\frac{R}{r_{\text{gal}}}\right)^{-3}, \tag{3.49}$$

where P_{gg} and P_{gc} are the perturbation parameters of galaxy-galaxy and galaxy-group interactions, respectively. While M_{comp} is the companion mass, M_{gal} represent the mass and r_{gal} is the visible radius of the galaxies, d refers to the separation between the two galaxies, M_{group} is the mass of the galaxy group, and R is the distance of the galaxy from the group center. The critical value of the perturbation parameters were defined by Byrd and Valtonen (1990) in range of $\geqslant 0.006$ to 0.1.